Synthesis and Characterization of Perovskite $Ca_{0.5}Sr_{0.5}MnO_3$ Nanoparticles in w/o-Microemulsions

A. López-Trosell* and R. Schomäcker*

* Department of Chemistry, TU-Berlin,TC 8
Strasse des 17. Juni 124, 10623-Berlin, Germany
Lopez.Alejandra@chem.tu-berlin.de and Schomaecker@tu-berlin.de

ABSTRACT

In the present work, w/o-microemulsions were employed to produce nanoparticles of perovskite ($Sr_{0.5}Ca_{0.5}MnO_3$) with an average diameter of 45 nm. The process was carried out via sol-gel in microemulsions. In order to control particle growth and distribution size, the micellar structure and synthesis conditions were investigated. Therefore, the phase behavior of the microemulsion systems were determined. Samples were characterized by X-ray diffraction (XRD), scanning electron microscopy (SEM), and N_2 adsorption.

Keywords: microemulsions, sol-gel, nanoparticles

1 INTRODUCTION

So-called perovskites are a large family of crystalline ceramics that derive their name from a specific mineral known as perovskite $CaTiO_3$. The unit cell of the cubic aristotype, represented for example by $CaTiO_3$ is type face-centred cubic. The space group is Pm3m. Using the general formula ABO_3, the large cations A occupy the corners of the cube (000), the small cation B the center ($\frac{1}{2}$ $\frac{1}{2}$ $\frac{1}{2}$), and the anions the center of the faces ($\frac{1}{2}$ $\frac{1}{2}$ 0, $\frac{1}{2}$ 0 $\frac{1}{2}$, 0 $\frac{1}{2}$ $\frac{1}{2}$). The ratio of the ionic radii is an important factor for the crystal structure. For non-ideal ratios, distortions from the cubic aristotype are observed [1].

The oxides of perovskite containing Mn ions have been the object of strong interest due to the exhibition of phenomena such as ferroelectricity, extremely high magnetoresistance, high-temperature O_2^--conductivity and high catalytic activity [2],[3],[4]. These properties have been found to be affected by the composition and particle size. More precisely, these properties show an increment when the particle sizes decrease. Therefore, the applied technique to control and to synthesize such materials is very important.

In the past, manganese perovskite have been obtained by conventional solid-stated synthesis. Unfortunately, this technique leads to solids with a larger grain size [5] due to the high-temperature treatment. In comparison with the solid-stated technique, microemulsions offer lower temperature conditions, which favor particle growth and avoid sintering processes. Reverse micelles have been successfully used to synthesize ultrafine particles (1-100 nm as grain diameter). Microemulsions are thermodynamically stable isotropic dispersions of two immiscible liquids consisting in microdomains of one of both liquids in the other, stabilized by an interfacial film of surfactant. These microdomains are used as microreactors, in which chemical reactions can be carried out. Consequently, they present a suitable medium to produce particles with desirable size and morphology. However, in order to control particle growth and distribution size, Schmidt [6], pointed out that not only the micellar structure is important but also the synthesis conditions and the kinetics of the elementary steps, especially the meterial exchange between the droplets.

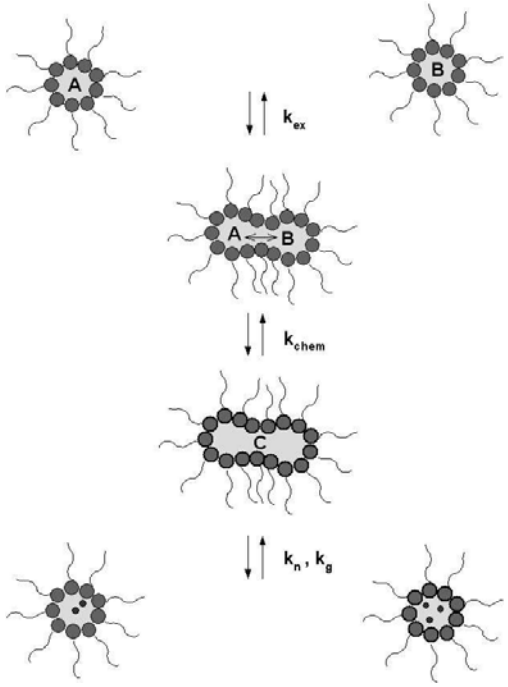

Figure 1: Schematic representation of the mechanism for formation of nanoparticles in w/o-microemulsion proposed by Schmidt. [6]

Several models have been proposed to explain the formation process of ultrafine particles in reverse micelles [7]–[11], [6]. On the one hand, there are some authors such as Tanori and Pileni [12], who suggest that micelles act as confined "nanoreactors", inside which the reaction takes place. They found that the size and form of the particles can be limited to

Table 1: Composition of the microemulsions used for the Perovskite synthesis. Microemulsion A (μE_A) and microemulsion B (μE_B) containing the salts and propionic acid, respectively. Ac denotes the acetate (CH_3COO^-).

	Surfactant	Oil phase	Aqueous phase
μE_A	Marlipal O13/70	cyclohexane	$Ca(Ac)_2$ + $Sr(Ac)_2$ [0.3] mol/l
			+ $Mn(Ac)_2$ [0.6] mol/l
μE_B	Marlipal O13/70	cyclohexane	$propionic\ acid$ [1.2] mol/l
Weight (g)	15	74.38	10.62

colloidal assemblies used as templates.

However, this mechanism seems to be contradicted by experiments that yielded particles larger than the droplets. On the other hand, authors like Towey [9] and Hirai [10] proposed models based on different stages of the precipitation reaction to explain the particle formation.

Figure 1 shows the possible kinetic scheme for the formation of the nanoparticles in reverse microemulsion based on the model proposed by Schmidt [6].

2 EXPERIMENTAL PART

The composition of microemulsions are specified by the weight fraction of oil in the mixture oil-water (α) and the weight fraction of surfactant in the ternary mixture (γ), where m_o, m_w and m_s are the weights of oil, water and surfactant, respectively.

$$\alpha = \frac{m_o}{(m_o + m_w)} \tag{1}$$

$$\gamma = \frac{m_s}{(m_o + m_w + m_s)} \tag{2}$$

An important parameter to describe the droplet size is the so-called "water pool", characterized by W_o. This parameter is the water-surfactant molar ratio (equation 3), which is considered to be proportional to the radius *R* of the droplet as was shown by Pileni [13].

$$W_o = \frac{n_w}{n_s} \tag{3}$$

Where n_w is the water mole and n_s is the surfactant mole.

For the nanoparticle synthesis, strontium acetate monohydrate ($Sr(CH_3COO)_2 \cdot H_2O$), calcium acetate monohydrate ($Ca(CH_3COO)_2 \cdot H_2O$) and mangan acetate tetrahydrate ($Mn(CH_3COO)_2 \cdot 4H_2O$) were employed. The acetates were supplied by Fluka with a purity $> 99\%$ and where used without further purifications. The propionic acid was suppled by Aldrich. Marlipal O13/70 (from Sasol) was used as surfactant. The number of carbons in the aliphatic chain as well as the ethoxylation degree are indicated by the label after the name, O13/70. This means that the surfactant has 13 carbons in the lipophilic chain and an average ethoxylation degree of seven. Cyclohexane was employed as oil phase. In order to determine the best microemulsion composition for preparing the precursor of Perovskite, the phase behavior of different systems was studied applying the procedure described in [14].

The synthesis of Perovskite $Ca_{0.5}Sr_{0.5}MnO_3$ was carried out via sol-gel in microemulsion. The reaction was achieved by using propionic acid as gelificant agent. Two microemulsions, "A" and "B", with identical composition but with different aqueous phases were prepared. In the microemulsion "A", the aqueous phase was a solution containing calcium acetate, strontium acetate, and mangan acetate in stoichiometric ratio, whereas the microemulsion "B" was a solution containing the propionic acid. The composition of the microemulsions is shown in table 1.

A semi-batch reactor was used to perform the synthesis of the perovskite. It consists of a tank with four baffles, and can contain $200\ ml$ of microemulsion as maximum. The agitator was a four pitched blade turbine impeller and the feed input was located near to the agitator and above the liquid level. The synthesis was achieved by loading $100\ ml$ of microemulsion "A" to the reactor and adding $100\ ml$ of other one at a constant feed rate and temperature, of $0.30\ (ml/s)$ and 27^oC, respectively. The temperature was controlled using a ultrathermostat K6 supplied by Colora Messtechnik. A peristaltic pump (Besta E100) was utilized for the addition of microemulsion "B" to the reactor.

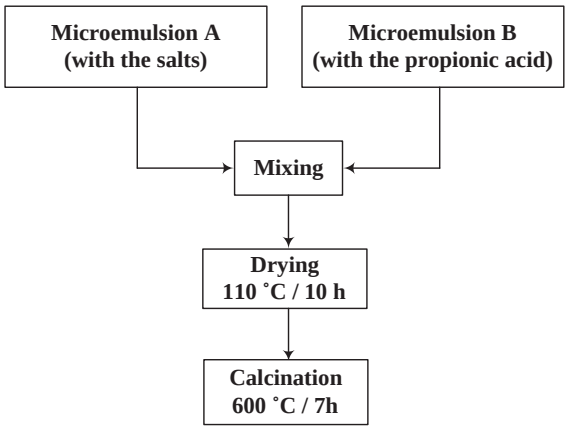

Figure 2: Diagram of the perovskite synthesis.

After addition, the reaction mixture was stirred for another 30 minutes. Subsequently, the solvents were removed by drying at 110^oC for 10 h. Afterwards, the precursor was calcined at different temperatures until the crystalline phase was obtained. The reaction was followed by XRD using a X-ray diffractometer Siemens D500 with Cu anode (radia-

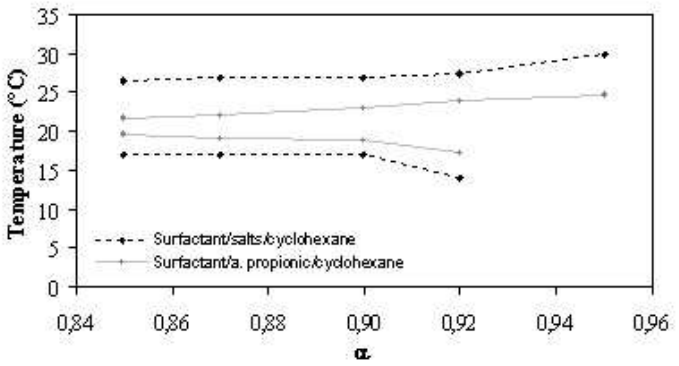

Figure 3: Phase diagram of the microemulsion systems.

tion $K_{\alpha 1}$ of $\lambda = 0.154\ nm$). The crystallized perovskite was analyzed by scanning electron microscopy (SEM) using a Hitachi S-520. The specific surface area was obtained from the N_2 adsorption (BET) using a Micromeritics Gemini with an analysis mode in equilibration, evacuation time of $1\ min$, equilibrium interval of $5\ sec$, and saturation pressure of $781.00\ mmHg$. Figure 2 presents a diagram of the employed synthesis process.

3 RESULTS AND DISCUSSIONS

Figure 3 shows the phase behavior of the microemulsion system water-oil-surfactant versus temperature. It is a typical phase diagram at a constant surfactant mass fraction (γ). The one phase region appears as a channel extending from the oil-rich region to the water-rich side of the diagram. In this region, the system is a thermodynamically stable dispersion, which is optically transparent and has a low viscosity.

The cyclohexane was chosen as oil component to prepare the system because its capacity to solubilize water in microemulsions is higher than with other oils such as hexane, octane and iso-octane as found in [6]. The results offer an extensive working range for temperature and composition of the microemulsions.

The X-ray patterns in figure 5 show that the sample reached the crystal structure by heat treatment at 600^oC for seven hours. The average crystall size D_{hkl} was calculated using the Debye-Scherrer's equation 4 with the full width at the half maximum β (in rad.) of the x-ray diffraction peak.

$$D_{hkl} = \frac{K\,\lambda}{\beta\,Cos\theta} \tag{4}$$

In the above equation K is a constant (often taken as 1), λ represents the X-ray wavelength, β and θ are the full width at the half maximum (in rad.) and the Bragg angle, respectively. The results calculated using Debye-Scherrer's equation are in good agreement with those obtained by SEM. Table 2 summarized the particle size obtained by XRD and SEM as well as the employed W_o.

Table 2: Particle diameters obtained by $^*XRD$ (D_{hkl}) and $^\ddagger SEM$ (D_p).

W_o	$*D_{hkl}\ nm$	$\ddagger D_p\ nm$
20	44	46

The SEM analysis (See figure 4) shows that the sample was homogeneous in shape and size. Finally, table 3 lists the specific surface area obtained by N_2 adsorption. This value is in the range of areas reported for some members of the manganite perovskite [4].

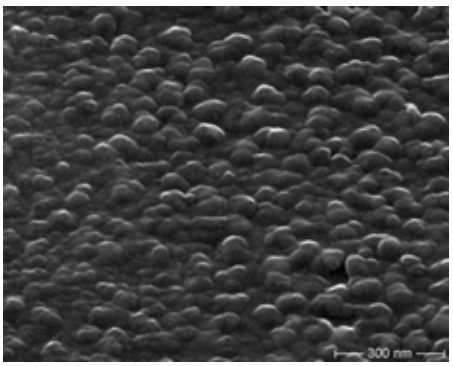

Figure 4: SEM of $Ca_{0.5}Sr_{0.5}MnO_3$ Perovskite.

Table 3: BET surface area (S_{BET}), Volume of pore (V_T) and diameter of pore (D_p) for the perovskite.

$S_{BET}\ (m^2/g)$	$V_T\ (cm^3/g)$	$D_p\ (nm)$
8.3	0.004	1.23

4 CONCLUSIONS

Microemulsion were used to synthesize $Ca_{0.5}Sr_{0.5}MnO_3$. Reverse micelles containg the adequate reactants are a suitable medium to obtain fine particles of perovskite with an av-

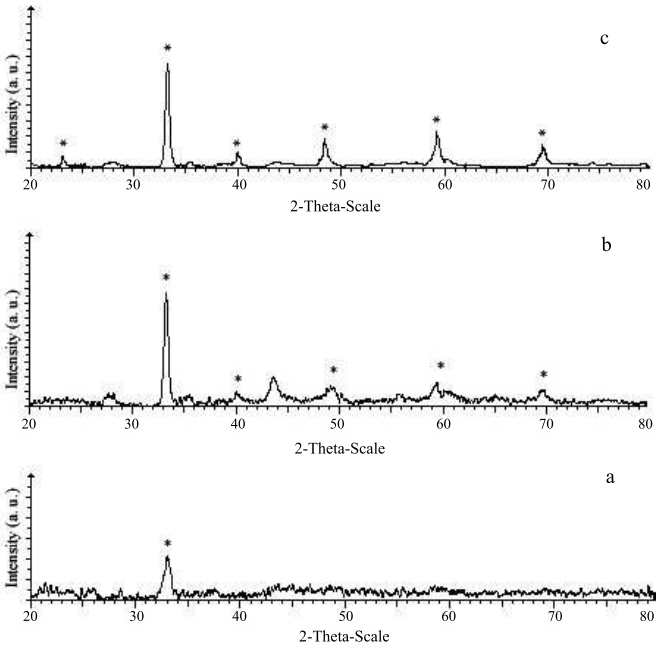

Figure 5: XRD patterns of $Ca_{0.5}Sr_{0.5}MnO_3$ Perovskite at different calcination conditions. (a) 2 h. at 300^oC, (b) 4 h. at 400^oC and (c) 7 h. at 600^oC.

erage diameter of $45\ nm$. The particles were homogeneous in size and shape and exhibited specific surfaces areas in the expected range.

REFERENCES

[1] Chmaissem, O., Dabrowski, B., Mais, J., Brown, D.E., Kruk, R., Prior, P., Jorgensen, J.D.: Relationship between structural parameters and the néll temperature in $sr_{1-x}ca_xmno_3$ $(0 \leq x \leq 1)$ and $sr_{1-y}ba_ymno_3$ $(y \leq 0.2)$. Physical Revew B **64** (2001) 1–9

[2] Galasso, S.F.: Structure, properties and preparation of perovskite type compounds. Pergamon Press: Oxford, Headington Hill Hall, Oxford, 4 and 5. Fitzroy Square, London W.1 (1969)

[3] Chen, C.H., Kruihof, H., Bouwmeester, H.J.M.: Ion conductivity of perovskite $laco_3$ measured by oxygen permeation technique. J. Applied Electrochemistry (1997) 71–75

[4] Song, K.S., Cui, H.X., Kim, S.D., Kang, S.K.: $la_{1-x}m_xmno_3$. Catalysis Today **47** (1999) 155–160

[5] Koch, C.C.: Nanostructured Materials- Processing Properties and Potential Applications. Carl C. Koch., NY (2002)

[6] Schmidt, J., Guesdon, C., Schomaecker, R.: Engineering aspects of preparation of nanocrystalline particles in microemulsion. J. Nanoparticle Reserch **1** (1999) 267–276

[7] Ravet, I., Nagy, J., Derouane, E.: On the mechanism of formation of colloidal monodisperse metal boride particles from reverse micelles composed of ctab-1-hexanol-water. Stud. Surf. Sci. Catal. **31** (1987) 505–516

[8] Osseo-Asare, K., Arriagada, F.: Synthesis of nanosize particles in reversed microemulsions. Ceram. Trans. **12** (1990) 3–16

[9] Towey, T., Khan-Lodhi, A., Robinson, B.: Kinetics and mechanism of formation in $water - aerosol - ot - oil$ microemulsions. J. Chem. Soc. Faraday Trans. **86** (1990) 3757–3762

[10] Hirai, T., Sato, H., Komasawa, I.: Mechamism of formation of titanium dioxide ultrafine particles in reverse micelles by hydrolysis of titanium tetrabutoxide. Ind. Eng. Chem. Res. **32** (1993) 3014–3019

[11] Bandoyopadhyaya, R., Kumar, R., Gandhi, K.: Modeling of precipitation in revese micellar systems. Langmuir **13** (1997) 3610–3620

[12] Tanori, J., Pileni, P.: Control of the shape of copper metallic particles by using a colloidal system as template. Langmuir **13** (1997) 639–646

[13] Pileni, M.P.: Reverse micelle as microreactors. J. Phys. Chem. (1993) 6961–6973

[14] Lade, M., Mays, H., Schmidt, J., Willumeit, R., Schomaecker, R.: On the nanoparticle synthesis in microemulsions: detailed characterization of an applied reaction mixture. Colloids and Surfaces A: Physicochem. Eng. Aspects **163** (2000) 3–15